Flexible NH₃ sensors fabricated by *in situ* self-assembly of polypyrrole

Pi-Guey Su *, Chi-Ting Lee, Cheng-Yi Chou

Department of Chemistry, Chinese Culture University, Taipei 111, Taiwan

ARTICLE INFO

ABSTRACT

Novel flexible NH₃ gas sensors were formed by the *in situ* self-assembly of polypyrrole (PPy) on plastic substrates. A negatively charged substrate was prepared by the formation of an organic monolayer (3-mercapto-1-propanesulfonic acid sodium salt—MPS) on a polyester (PET) substrate using a pair of comb-like Au electrodes. Two-cycle poly(4-styrenesulfonic acid) sodium salt/poly(allylamine hydrochloride) (PSS/PAH) bilayers (precursor layer) were then layer-by-layer (LBL) deposited on an MPS-modified substrate. Finally, a monolayer of PPy self-assembled *in situ* and PPy multilayer thin films self-assembled LBL *in situ* on a (PSS/PAH)₂/MPS/Au/Cr/PET substrate. The thin films were analyzed by atomic force microscopy (AFM). The effects of the precursor layer (PSS), the deposition time of the monolayer of PPy and the number of PPy multilayers on the gas sensing properties (response) and the flexibility of the sensors were investigated to optimize the fabrication of the film. Additionally, other sensing properties such as sensing linearity, reproducibility, response and recovery times, as well as cross-sensitivity effects were studied. The flexible NH₃ gas sensor exhibited a strong response that was comparable to or even greater than that of sensors that were fabricated on rigid substrate at room temperature.

© 2009 Elsevier B.V. All rights reserved.

1. Introduction

The fabrication of organic electronic devices on plastic substrates has attracted much interest recently, because of the proliferation of handheld portable consumer electronics. Plastic substrates have many attractive characteristics, such as biocompatibility, flexibility, lightness, shock resistance, softness and transparency [1]. A new trend towards the direct integration of sensors on flexible substrates has become evident. Flexible multisensor platforms that support temperature, humidity and gas detection will be manufactured at very low-cost and integrated into smart textiles or radio frequency identification (RFID) tags for logistics applications [2,3]. The development of sensors should be consistent with the future goal of the development of the completely plastic RFID tag, and extensible to the sensing of various gases. The main challenge is not only their manufacture, but also the stability of their mechanical, electrical and gas sensing properties.

Conducting polymers such as polythiophene, polypyrrole (PPy) and polyaniline have been intensively studied because of their remarkable mechanical and electrical properties, which can be exploited in actuators, sensors and electrochromic devices [4–6]. Among conducting polymers, PPy has attracted much particular interest because it is easily synthesized; it has relatively good environmental stability, and its surface charge characteristics can easily

be modified by changing the dopant species in the material during synthesis.

Many approaches for fabricating PPy films have been proposed. They include chemical deposition by dip-coating [6,7], vapor deposition polymerization [8], UV-photopolymerization [9], deposition of Langmuir–Blodgett film [10], and electrochemical deposition [11,12]. The layer-by-layer (LBL) self-assembly of multilayer films based on sequential adsorptions of ionized polyelectrolytes and oppositely charged materials in aqueous solutions has been developed [13,14]. LBL self-assembly has many advantages over other methods, including simplicity, low-cost, low temperature of deposition, controllable thickness (from nanometers to micrometers) and the lack of any need for complex equipment. Therefore, the preparation of PPy multilayered films using LBL and *in situ* self-assembly has been studied [15–18]. Notably, the surfaces coated by PPy in these studies were deposited on rigid substrates, such as ceramics or SiO₂/Si. Recently, Ferrer-Anglada et al. [19] adopted the electrochemical method to prepare PPy and polyaniline on plastic substrate as a pH sensor. However, no attempt has been made to form a flexible NH₃ gas sensor based on PPy thin films by LBL *in situ* self-assembly. In this work, flexible NH₃ gas sensors were fabricated by the *in situ* self-assembly of monolayer of PPy and the LBL *in situ* self-assembly of PPy multilayer thin films on a flexible substrate (polyester film—PET). Poly(styrenesulfonic acid) sodium salt (PSS) assembled with poly(allylamine hydrochloride) (PAH) was a precursor layer before the PPy thin film was self-assembled *in situ*. The thin films were observed by atomic force microscopy (AFM). The effects of the precursor layer (PSS), the deposition time

---

* Corresponding author. Tel.: +886 2 28610511x25332; fax: +886 2 28614212.
E-mail address: spg@faculty.pccu.edu.tw (P.-G. Su).

of the monolayer of PPy and the number of PPy multilayers on the gas sensing properties (response) and the flexibility of the sensors were investigated. The other gas sensing properties, such as sensing linearity, reproducibility, response and recovery times, as well as cross-sensitivity effects were also investigated.

2. Experimental

2.1. Materials

3-Mercapto-1-propanesulfonic acid sodium salt (MPS), poly(allylamine hydrochloride) (PAH; Mw = 15,000), poly-(styrenesulfonic acid) sodium salt (PSS; Mw = 70,000), pyrrole monomer (98%), *p*-toluene sulfonic acid (*p*-TSA) and ferric chloride (FeCl$_3$) were obtained from Aldrich. All used deionized water (DIW) were prepared using a Milli-Q Millipore (Bedford, MA, USA) purification system, and the resistivity of water was above 18.0 MΩ/cm.

2.2. Preparation of substrates

The structure of the flexible NH$_3$ gas sensors was the same as that in our earlier study [20]. The interdigited gold electrodes (IDE) were made by sputtering first Cr (50 nm thick) and then Au (250 nm thick) at temperature from 120 to 160 °C. The gap between electrodes was 0.2 mm. The substrates were first immersed in a bath that contained a solution of H$_2$O$_2$/H$_2$SO$_4$ (1:2 volume ratio) for 3 min. The substrates were thoroughly rinsed with DIW after each step. This process made the substrates hydrophilic. The negatively charged MPS/Au surface was prepared by immersing the hydrophilic Au/Cr/PET substrate in 2.0 mM aqueous MPS for 24 h, rinsing it with DIW and then drying it at 80 °C. A cyclic PSS/PAH bilayer film architecture was produced by alternately depositing PAH (pH 4) and PSS (pH 1) aqueous solution onto the negatively charged MPS-modified substrate. For each layer produced, the immersion time was about 10 min and rinsing and drying followed each immersion. Therefore, a two-cycle PSS/PAH bilayers film was fabricated by repeating the above processes, yielding, a negatively charged (PSS/PAH)$_2$/MPS/Au/Cr/PET substrate.

2.3. Preparation of monolayer of PPy and PPy multilayered films

The active solution for use in PPy contained the oxidizing agent (FeCl$_3$) and *p*-TSA, and was later adjusted to pH 1 by adding HCl; then the pyrrole monomer was added. The optimal film of PPy was produced using a solution of 0.006 M FeCl$_3$, 0.026 M *p*-TSA and 0.02 M pyrrole, as described in the literature [16,18]. The active solution was stirred for 15 min. A monolayer PPy was self-assembled *in situ* as a thin film on the (PSS/PAH)$_2$/MPS/Au/Cr/PET substrate. The PPy multilayered thin films, composed of (PPy/PSS)$_n$, were deposited on the (PSS/PAH)$_2$/MPS/Au/Cr/PET substrate in the same manner as the PSS/PAH multilayered thin films, where *n* is the number of coated layers. The optimal deposition time in PPy active solution and PSS solution was 5 and 10 min, respectively. Table 1 presents the various compositions of interest. Fig. 1(a) schematically depicts an *in situ* self-assembly of a PPy monolayer film on PET substrate over time. Fig. 1(b) schematically depicts an LBL *in situ* self-assembly of a PPy/PSS multilayered thin film on a PET substrate. Fig. 2 presents the flexibility of the PPy multilayer thin film assembled on a PET substrate.

2.4. Instruments and analysis

The surface microstructure of the thin film that was coated on a PET substrate was investigated using a field emission scanning electron microscope (FE-SEM, JEOL, JSM 6335F) and an atomic force

Table 1
Compositions of precursor layer and PPy thin films used to prepare flexible NH$_3$ sensors.

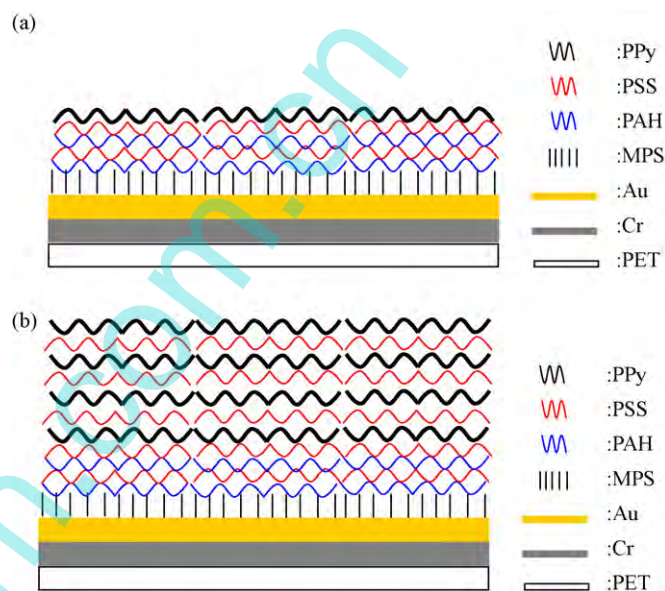| Sample number	Precursor layer	PPy layer	
	PSS concentration (mg/mL)	Deposition time (min)	Numbers of PPy/PSS bilayer
1	0.5	5	1
2	1	5	1
3	2	5	1
4	1	10	1
5	1	15	1
6	1	30	1
7	1	5	2
8	1	5	5

Fig. 1. Schematic diagram of PPy thin films assembled *in situ* on modified PET substrate; (a) *in situ* self-assembly of monolayer of PPy on PSS surface at various times and (b) LBL *in situ* self-assembly of PPy with PSS.

Fig. 2. Photograph of bent flexible NH$_3$ gas sensor based on PPy thin film assembled *in situ* on modified PET substrate.
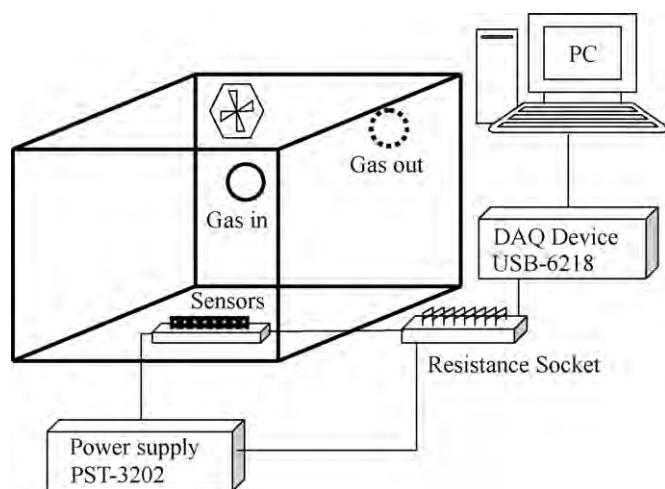
Fig. 3. Measurement system for testing gas sensors.

microscope (AFM, Ben-Yuan, CSPM 4000) in tapping mode. The electrical and sensing charactersteristics were measured using a bench system at room temperature, as shown in Fig. 3. Each sensor was connected in series with a load resistor and a fixed 5 V was continuously supplied to the sensor circuit from a power supply (GW, PST-3202). The resistance of the sensor was determined from the voltage at the ends of the load resistor using a DAQ device (NI, USB-6218) in various concentrations of gas. The desired NH_3 gas concentrations, obtained by mixing a known volume of standard NH_3 gas (100,000 ppm) with N_2, were injected into the chamber. The cross-sensitivity experiment was performed by measuring the resistance of the sensor upon controlled concentration of 5, 200 and 1000 ppm for NO_2, CO and H_2 gases, respectively. The gas inside the chamber was uniformly distributed using a fan. After some time, the chamber was purged with air and the experiment was repeated for another cycles. All experiments were performed at room temperature, and the relative humidity was 53 ± 3 RH%. Flexibility experiments were performed in which the sensors were bent to various degrees as their responses were monitored as a function of the period of exposure to NH_3 gas. The bending angle was measured using a goniometer.

3. Results and discussion

3.1. Microstructure of surface

Fig. 4 presents the surface morphology of the *in situ* self-assembled of manolayer of PPy and PPy multilayered thin films on a modified PET substrate, analyzed using tapping-mode AFM. The size of each image is $5 \mu m \times 5 \mu m$. Table 2 presents the roughness and sphere size of various PPy thin films that were deposited on the modified PET substrate. Fig. 4(a)–(c) (Samples 1–3) presents the surface morphology of *in situ* self-assembled films of a mono-

Table 2
Roughness and sphere size of various PPy thin films deposited on a modification of PET substrate.

Sample number	RMS (nm)	Size cluster circular (Φ) (nm)
1	10.6	58 ± 25
2	12.4	50 ± 22
3	11.7	53 ± 25
4	14.8	52 ± 30
5	20.1	68 ± 47
6	35.3	78 ± 42
7	38.0	74 ± 50
8	42.6	82 ± 60

layer of PPy fabricated on a modified PET substrate using various PSS concentrations. The PPy films all had typical granular patterns and the size of spheres ranged from 50 to 58 nm. Fig. 4(a) (Sample 1) indicates that less PPy *in situ* self-assembled as films on modified PET substrate than in Samples 2 and 3 (Fig. 4(b) and (a)) because the charge on the previously grown layer of Sample 1 was lower than that of Samples 2 and 3. Therefore, Sample 1 exhibited some imperfections in packing. Fig. 4(b) and (d)–(f) (Samples 2 and 4–6) presents the surface morphologies of the *in situ* self-assembled films of monolayers of PPy at various times. Clearly, the surface roughness and sphere size increased from 12.4 to 35.3 and from 50 to 78 nm, respectively, as the deposition time of the monolayer of PPy increased. The films of PPy were completely covered with fine grains after 5 min. Fig. 4(b), (g) and (h) (Samples 2, 7 and 8) presents the surface morphologies of LBL *in situ* self-assembled films of PPy multilayers for various numbers of PPy/PSS bilayers. The surface topography of the alternate PPy and PSS deposited LBL film reveals a similar structure is similar to that of monolayer of PPy films. The size of the spheres of PPy multilayered exceeded that of single-layered PPy thin films. The surface roughness and sphere size increased from 12.4 to 42.6 and from 50 to 82 nm, respectively, as the number of PPy/PSS bilayers increased. This difference between the surface morphologies of the *in situ* self-assembled monolayer of PPy and the PPy multilayered thin films may be associated with the different molecular orientations of PPy [16,17].

3.2. Flexibility and response properties of monolayer of PPy and PPy multilayered thin films

Fig. 5 plots the effect of the concentration of PSS, the deposition time of the monolayer of PPy and the number of PPy/PPS bilayers in the *in situ* self-assembled PPy thin films on their flexibility characteristics. At each bending angle, the sensors were exposed to 50 ppm NH_3 gas. Table 3 presents the corresponding responses. The sensor response (*S*) was given by $S = (R_{gas} - R_{air})/R_{air}$ ($\Delta R/R_{air}$), where R_{gas} and R_{air} are the electrical resistances of the sensor in the tested gas and air, respectively.

3.2.1. Effect of concentration of PSS on flexibility and response of monolayer of PPy thin films

Fig. 5(a) plots the effect of the concentration of PSS on the flexibility characteristics of the *in situ* self-assembled PPy thin monolayer films. When the concentration of PSS exceeded 1 mg/mL, the deviations of the responses of Samples 2 and 3 were both under 10% when the sensors were bent downward at an angle of up to 60° from horizontal. In the LBL *in situ* self-assembly process, before the PPy monolayer and the PPy/PSS multilayered coating systems were constructed, two-cycle PSS/PAH bilayers (precursor layer) were deposited on the MPS-modified substrate to improve the combinability of the surface and the first monolayer of the film of PPy. Additionally, the polyanion PSS layer on the substrates is importantly involved in the formation of the PPy thin film, which involves the simultaneous polymerization of the pyrrole monomer and oxidation of the PPy molecules [16–18]. Therefore, in a more dilute PSS solution, less charge remained on the previously grown layer, and so less Fe^{3+} is adsorbed on the PSS, causing poorer polymerization of PPy on the surface [16]. In a more concentrated PSS solution, some PPy molecules aggregate and become entangled with each other (as observed in Fig. 4(c)), increasing the size of the spheres. Therefore, Sample 2 had a higher response than Sample 3 (Table 3).

3.2.2. Effect of deposition time of PPy on flexibility and response of monolayer of PPy thin films

Fig. 5(b) plots the effect of deposition time of PPy on the flexibility characteristics of the *in situ* self-assembled monolayer of PPy
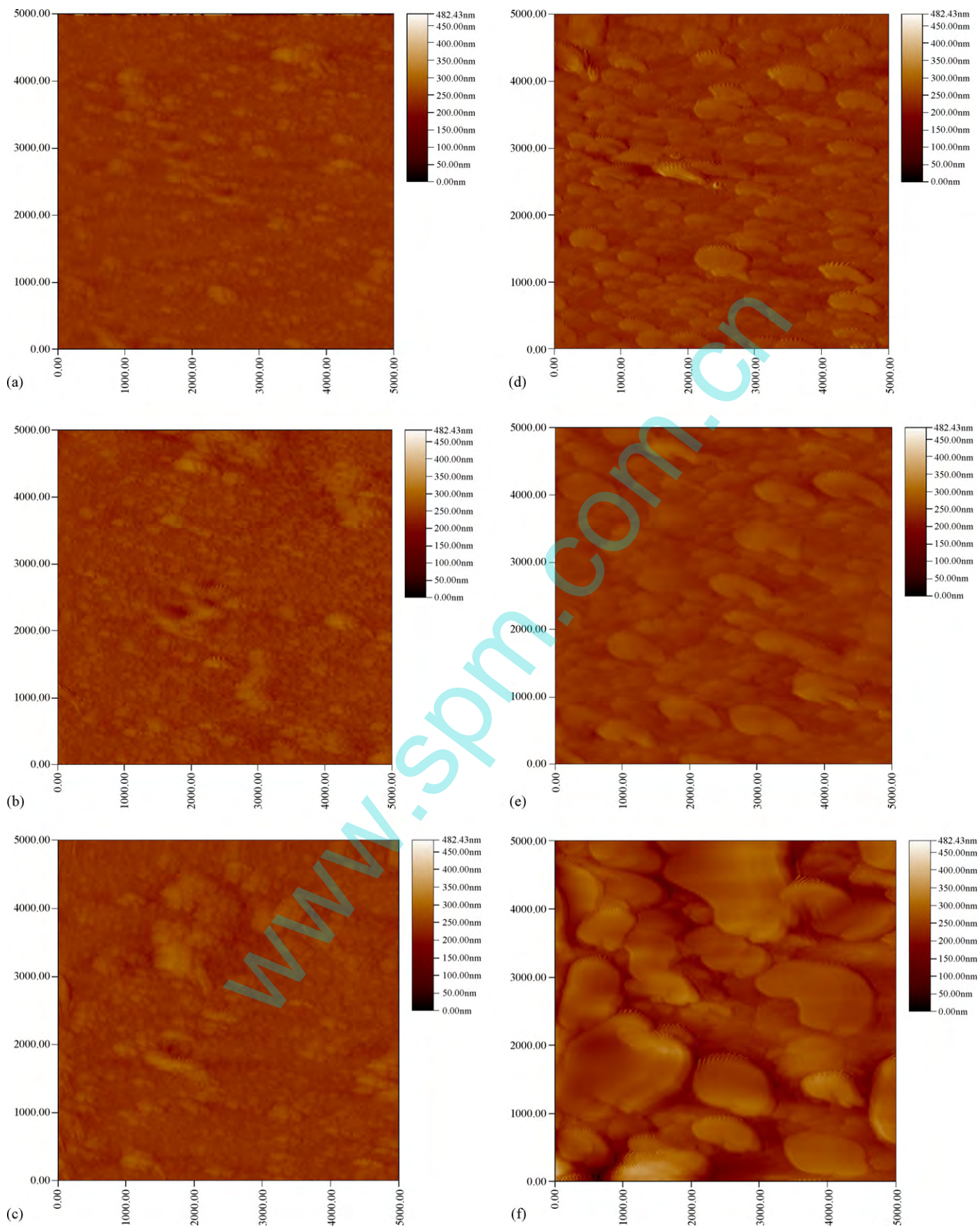
Fig. 4. AFM micrographs of various PPy thin films assembled *in situ* on modified PET substrate (compositions as shown in Table 1); (a) Sample 1, (b) Sample 2, (c) Sample 3, (d) Sample 4, (e) Sample 5, (f) Sample 6, (g) Sample 7 and (h) Sample 8.
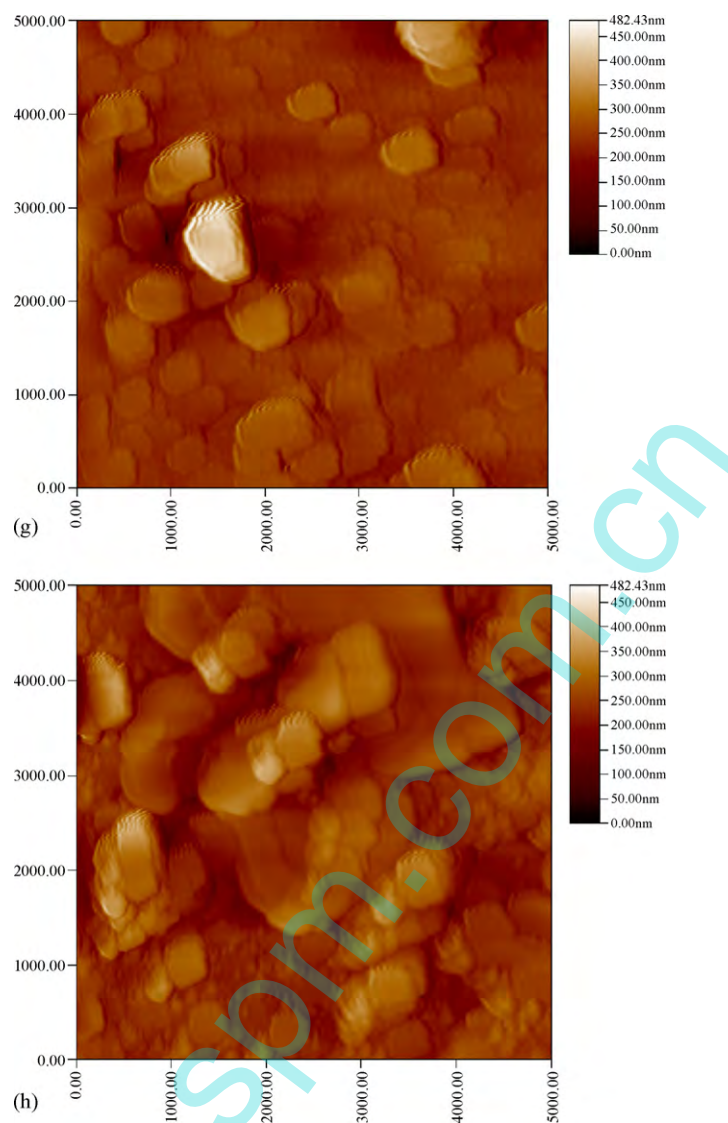
(g)

(h)

Fig. 4. (*Continued*).

thin films. When the sensors were bent downward at an angle of up to 60° from horizontal, the response deviation increased with the deposition time of the monolayer of PPy on a modified PET substrate increased (Samples 2 and 4–6). In the LBL *in situ* self-assembly process, the PSS layer, acting as an intermediate electrostatic adhesive, helped to maintain the positions of PPy, even when the substrate was bent. Consequently, a large PPy adheres to the PET surface less strongly than a small PPy (as observed in Figs. 4(b) and (d)–(f);

Table 3
Response to NH_3 of various PPy thin films deposited on a modification of PET substrate.

Sample number	Response[a]
1	42.66
2	77.75
3	58.01
4	54.76
5	38.40
6	29.38
7	33.40
8	29.33

[a] Sensor response at 50 ppm NH_3 gas.

Table 2). The sensor response decreased as the deposition time of the monolayer of PPy on the modified PET substrate increased (Table 3). Therefore, PPy in the thin film assemblies was small, so the surface area was large, favoring the adsorption of gas molecules.

3.2.3. Effect of number of PPy/PPS bilayers on flexibility and response of PPy multilayer thin films

Fig. 5(c) plots the effect of the number of PPy/PPS bilayers on the flexibility of the LBL *in situ* self-assembled PPy multilayer thin films. In the PPy/PSS multilayer thin film, PPy was reinforced by two adjacent PSS layers as intermediate electrostatic glue and therefore, the PSS molecules helped to keep the PPy in their positions even when the substrate was bent. However, the spheres of multilayered PPy were too large to adhere to the PET surface when the substrate was bent (as observed in Fig. 4(b), (g) and (h); Table 2). Therefore, the $(PPy/PSS)_1$ multilayer thin film (Sample 2) was more flexible than that of $(PPy/PSS)_2$ (Sample 7) and $(PPy/PSS)_5$ (Sample 8). The sensor response decreased as the number of PPy/PPS bilayers increased (Table 3). This result was reasonable because of the effect of the size of PPy (as described in Section 3.2.2). Sample 2 showed the highest response (77.75) and greatest flexibility (within 8%), and so Sample 2 was chosen to study the other gas sensing properties.
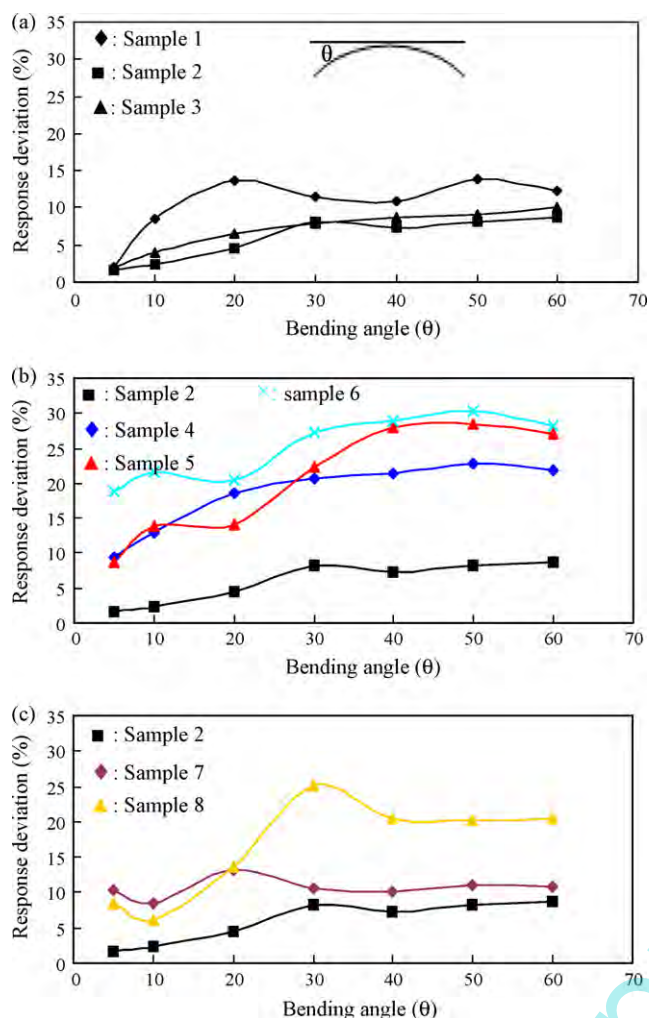
Fig. 7. Response (S) of Sample 2 sensor as function of concentration of NH$_3$ gas (with compositions as shown in Table 1).

Table 4
Linear sensing characteristics of Sample 2 sensor at different concentrations of NH$_3$ gas.

Concentration (ppm)	Sensing characteristics	
	Slope	Linearity[a]
5–50	1.036	0.9857
50–200	0.1646	0.9996

[a] Correlation coefficient.

was observed from 50 to 200 ppm of NH$_3$ gas. This behavior was related to the adsorption of NH$_3$ gas molecules on the surface of the PPy film. Therefore, at the concentration of NH$_3$ increased (50–200 ppm), suggesting the absence of active sites for adsorption, causing the steep decrease in the slope. Therefore, the respondent sensitivity of Sample 2 to a low concentration of NH$_3$ gas was much higher than that to a high concentration of NH$_3$ gas. The NH$_3$ gas sensing properties of the present flexible NH$_3$ sensor were compared with the sensor fabricated on rigid substrate in Table 5. The response of Sample 2 exceeded that of sensors made from electrosynthesized and chemical polymerized PPy film on Al$_2$O$_3$ or SiO$_2$ substrate: Sample 2 had a detection limit of 5 ppm of NH$_3$ gas [10,21–26]. Fig. 8 plots the real-time response of Sample 2. The response (RT$_{90}$) and recovery time of Sample 2 were 12 and 52 s, respectively, at the testing concentration of 50 ppm of NH$_3$. Moreover, five gas on/off cycles produced similar responses, indicating the reproducibility of Sample 2. Table 6 presents the results on the cross-sensitivity effects of NO$_2$, CO and H$_2$ gases on the sensor. NO$_2$, CO and H$_2$ gases may be regarded as having undesirable cross-sensitivity effects with NH$_3$.

Fig. 5. Flexibility of various PPy thin films assembled *in situ* on modified PET substrate in response to 50 ppm NH$_3$ gas (compositions as shown in Table 1): (a) effect of concentration of PSS, (b) effect of deposition time of monolayer of PPy and (c) effect of number of PPy/PPS bilayers.

3.3. Gas sensing characteristics of flexible gas sensor

Fig. 6 plots the responses of Sample 2 to various concentrations of NH$_3$. Fig. 7 plots the results of calibration curve of Sample 2, and the slope and linear correlation coefficient were calculated, as shown in Table 4. The linear sensing characteristics in the ranges 5–50 ppm and 50–200 ppm differed. A steep decrease in slope
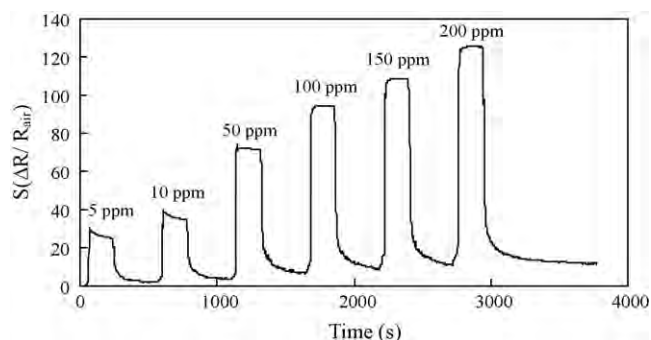

Fig. 6. Response (S) as a function of time (s) for various concentrations of NH$_3$ gas on Sample 2 sensor (with compositions as shown in Table 1).
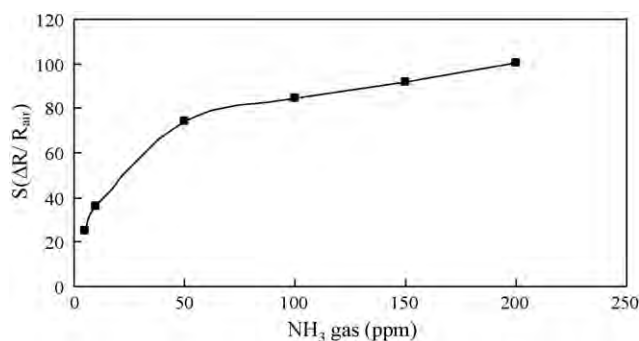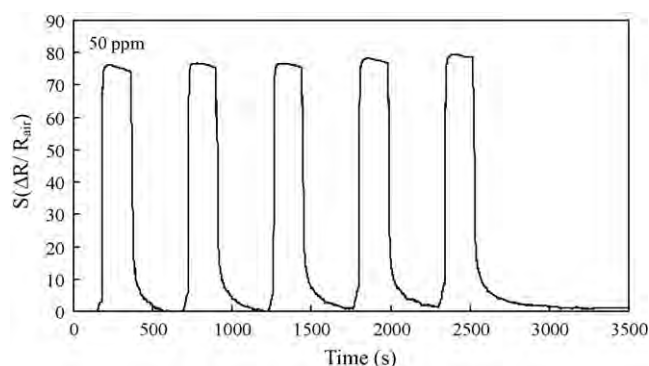

Fig. 8. Reproducibility of response of Sample 2 sensor to NH$_3$ gas (with compositions as shown in Table 1).

Table 5
Flexible NH_3 sensor performance of this work compared with the literatures.

Sensor substrate	Sensing material	Fabrication method	Detection limit (ppm)	References
PET	PPy	LBL self-assembly	5	This work
Glass	PPy–LiClO$_4$	Electrochemical deposition	10	[21]
Glass	PPy	Langmuir–Blodgett	100	[10]
Al$_2$O$_3$	PPy/poly(vinyl alcohol)	Electrochemical deposition	50	[22]
Glass	polypyrrole/sulfonated polyaniline	Electrochemical deposition	20	[23]
Glass	PPy/carbon nanofiber	Vapor deposition polymerization	10	[24]
SiO$_2$	PPy/single walled carbon nanotubes	Chemical oxidation	10	[25]
SiO$_2$	PPy	Electrochemical deposition	8	[26]

Table 6
Response (S) of Sample 2 sensor to various gases.

NH$_3$ (50 ppm)	NO$_2$ (5 ppm)	CO (200 ppm)	H$_2$ (1000 ppm)
77.75	19.16	0.21	0.46

4. Conclusions

A novel flexible NH_3 gas sensor was successfully fabricated by layer-by-layer *in situ* self-assembly of a PPy thin film on a modified PET substrate. The gas sensing properties (response) and flexibility characteristics of the fabricated sensors depended strongly on the architecture of the PPy layer. A precursor layer was optimally fabricated with 1 mg/mL concentration of PSS, a deposition time of PPy of 5 min and an *in situ* self-assembled monolayer PPy thin film for use in a novel flexible NH_3 gas sensor for future low-cost and flexible applications. The novel flexible NH_3 gas sensor had very high flexibility, a very high response and acceptable linearity ($R^2 = 0.9976$) between 5 and 50 ppm, a very fast response (12 s), a short recovery time (52 s), high reproducibility and an undesirable cross-sensitivity effect. The flexible NH_3 gas sensor exhibited a sensing performance that is comparable to or even greater than that of the sensors fabricated on the rigid substrate at room temperature.

Acknowledgements

References

[1] M.C. Mcalpine, H. Ahmad, D. Wang, J.R. Heath, Nat. Mater. 16 (2007) 379.
[2] E. Abad, S. Zampolli, S. Macro, A. Scorzoni, B. Mazzolai, A. Juarros, D. Gómez, I. Elmi, G.C. Cardinali, J.M. Gómez, F. Palacio, M. Cicioni, A. Mondini, T. Becker, I. Sayhan, Sens. Actuators B 127 (2007) 2.
[3] A. Vergara, E. Llobet, J.L. Ramírez, P. Ivanov, L. Fonseca, S. Zampolli, A. Scorzoni, T. Becker, S. Marco, J. Wöllenstein, Sens. Actuators B 127 (2007) 143.
[4] E. Smela, J. Micromech. Microeng. 9 (1999) 1.
[5] R.H.M. van de Leur, A. van der Waal, Syn. Met. 102 (1999) 1330.
[6] J.H. Cho, J.B. Yu, J.S. Kim, S.O. Sohn, D.D. Lee, J.S. Huh, Sens. Actuators B 108 (2005) 389.
[7] S. Brady, K.T. Lau, W. Megill, G.G. Wallace, D. Diamond, Syn. Met. 154 (2005) 25.
[8] E. Stussi, S. Cella, G. Serra, G.S. Venier, Mater. Sci. Eng. C 4 (1996) 27.
[9] P.G. Su, L.N. Huang, Sens. Actuators B 123 (2007) 501.
[10] M. Penza, E. Milella, M.B. Alba, A. Quirini, L. Vasanelli, Sens. Actuators B 40 (1997) 205.
[11] Q. Fang, D.G. Chetwynd, J.A. Covington, C.S. Toh, J.W. Gardner, Sens. Actuators B 84 (2002) 66.
[12] J.N. Barisci, G.G. Wallace, M.K. Andrews, A.C. Partridge, P.D. Harris, Sens. Actuators B 84 (2002) 252.
[13] G. Decher, J.D. Hong, J. Schmitt, Thin Solid Films 210 (1992) 831.
[14] G. Decher, Science 277 (1997) 1232.
[15] A.C. Fou, M.F. Rubner, Macromolecules 28 (1995) 7115.
[16] M.K. Ram, M. Adami, P. Faraci, C. Nicolini, Polymer 41 (2000) 7499.
[17] M. Onoda, K. Tada, A. Shinkuma, Thin Solid Films 499 (2006) 61.
[18] H. Tai, Y. Jiang, G. Xie, J. Yu, M. Zhao, Intern. J. Environ. Anal. Chem. 87 (2007) 539.
[19] N. Ferrer-Anglada, M. Kaempgen, S. Roth, Phys. Stat. Sol. 243 (2006) 3519.
[20] P.G. Su, C.S. Wang, Sens. Actuators B 123 (2007) 1071.
[21] M. Brie, R. Turcu, C. Neamtu, S. Pruneanu, Sens. Actuators B 37 (1996) 119.
[22] C.W. Lin, B.J. Hwang, C.R. Lee, Mater. Chem. Phys. 58 (1999) 114.
[23] H. Bai, Q. Chen, C. Li a, C. Lu, G. Shi, Polymer 48 (2007) 4015.
[24] J. Jang, J. Bae, Sens. Actuators B 122 (2007) 7.
[25] N.V. Hieu, N.Q. Dung, P.D. Tam, T. Trung, N.D. Chien, Sens. Actuators B 140 (2009) 500.
[26] S. Carquigny, J.B. Sanchez, F. Berger, B. Lakard, F. Lallemand, Talanta 78 (2009) 199.